University of Bristol - Explore Bristol Research
General rights

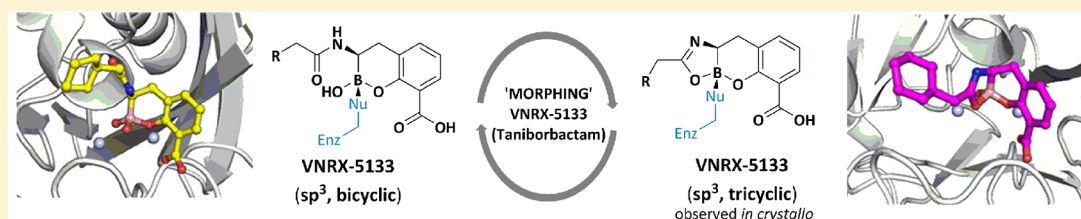# Bicyclic Boronate VNRX-5133 Inhibits Metallo- and Serine-β-Lactamases

Alen Krajnc,[†] Jürgen Brem,[†] Philip Hinchliffe,[‡] Karina Calvopiña,[†] Tharindi D. Panduwawala,[†] Pauline A. Lang,[†] Jos J. A. G. Kamps,[†] Jonathan M. Tyrrell,[§] Emma Widlake,[§] Benjamin G. Saward,[†] Timothy R. Walsh,[§] James Spencer,[‡] and Christopher J. Schofield*,[†]

[†]Chemistry Research Laboratory, Department of Chemistry, University of Oxford, 12 Mansfield Road, Oxford OX1 3TA, United Kingdom

[‡]School of Cellular and Molecular Medicine, Biomedical Sciences Building, University Walk, University of Bristol, Bristol BS8 1TD, United Kingdom

[§]Department of Medical Microbiology & Infectious Disease, Institute of Infection & Immunity, UHW Main Building, Heath Park, Cardiff CF14 4XN, United Kingdom

S *Supporting Information*

ABSTRACT: The bicyclic boronate VNRX-5133 (taniborbactam) is a new type of β-lactamase inhibitor in clinical development. We report that VNRX-5133 inhibits serine-β-lactamases (SBLs) and some clinically important metallo-β-lactamases (MBLs), including NDM-1 and VIM-1/2. VNRX-5133 activity against IMP-1 and tested B2/B3 MBLs was lower/not observed. Crystallography reveals how VNRX-5133 binds to the class D SBL OXA-10 and MBL NDM-1. The crystallographic results highlight the ability of bicyclic boronates to inhibit SBLs and MBLs via binding of a tetrahedral (sp³) boron species. The structures imply conserved binding of the bicyclic core with SBLs/MBLs. With NDM-1, by crystallography, we observed an unanticipated VNRX-5133 binding mode involving cyclization of its acylamino oxygen onto the boron of the bicyclic core. Different side-chain binding modes for bicyclic boronates for SBLs and MBLs imply scope for side-chain optimization. The results further support the "high-energy-intermediate" analogue approach for broad-spectrum β-lactamase inhibitor development and highlight the ability of boron inhibitors to interchange between different hybridization states/binding modes.

INTRODUCTION

β-Lactamase-catalyzed hydrolysis is the most important resistance mechanism for β-lactams, which comprise the most important class of antibacterials (Figure 1A, top).[1] Inhibitors of one of the two mechanistic classes of β-lactamases, the nucleophilic serine-β-lactamases (SBLs),[2] are established drugs for use in combination with an appropriate β-lactam antibiotic partner (Figure 1B, bottom). The well-established SBL inhibitors (clavulanic acid,[3,4] sulbactam,[5] tazobactam[6]) only inhibit a subset of SBLs (Ambler class A and some class C enzymes, but not typically class D enzymes) and are increasingly susceptible to evolved resistance, including via bacterial production of extended-spectrum serine-β-lactamases (ESBLs). The same issues are compromising the use of carbapenems, which manifest both antibacterial and β-lactamase inhibition properties.[7,8]

The clinical importance of the second mechanistic class of β-lactamases, i.e., the zinc-ion-dependent metallo-β-lactamases (MBLs), which have a different fold/evolutionary origin to the SBLs, is growing.[9] This is of particular concern because MBLs catalyze the efficient hydrolysis of nearly all β-lactam classes, with the exception of the monobactams, which are not currently hydrolyzed by MBLs at a clinically relevant rate.[10] The vulnerability of the β-lactams to β-lactamases has long stimulated interest in developing non-β-lactam inhibitors of penicillin-binding proteins (PBPs) and β-lactamases. These studies resulted in the development of avibactam,[11,12] which, unlike (at least most) "traditional" β-lactam inhibitors that act irreversibly to form acyl-enzyme complexes, inhibits class A, C, and some class D SBLs by reversible formation of an acyl-enzyme-type complex via reaction of its diazabicyclooctane core. However, avibactam does not inhibit MBLs;[13] moreover, there
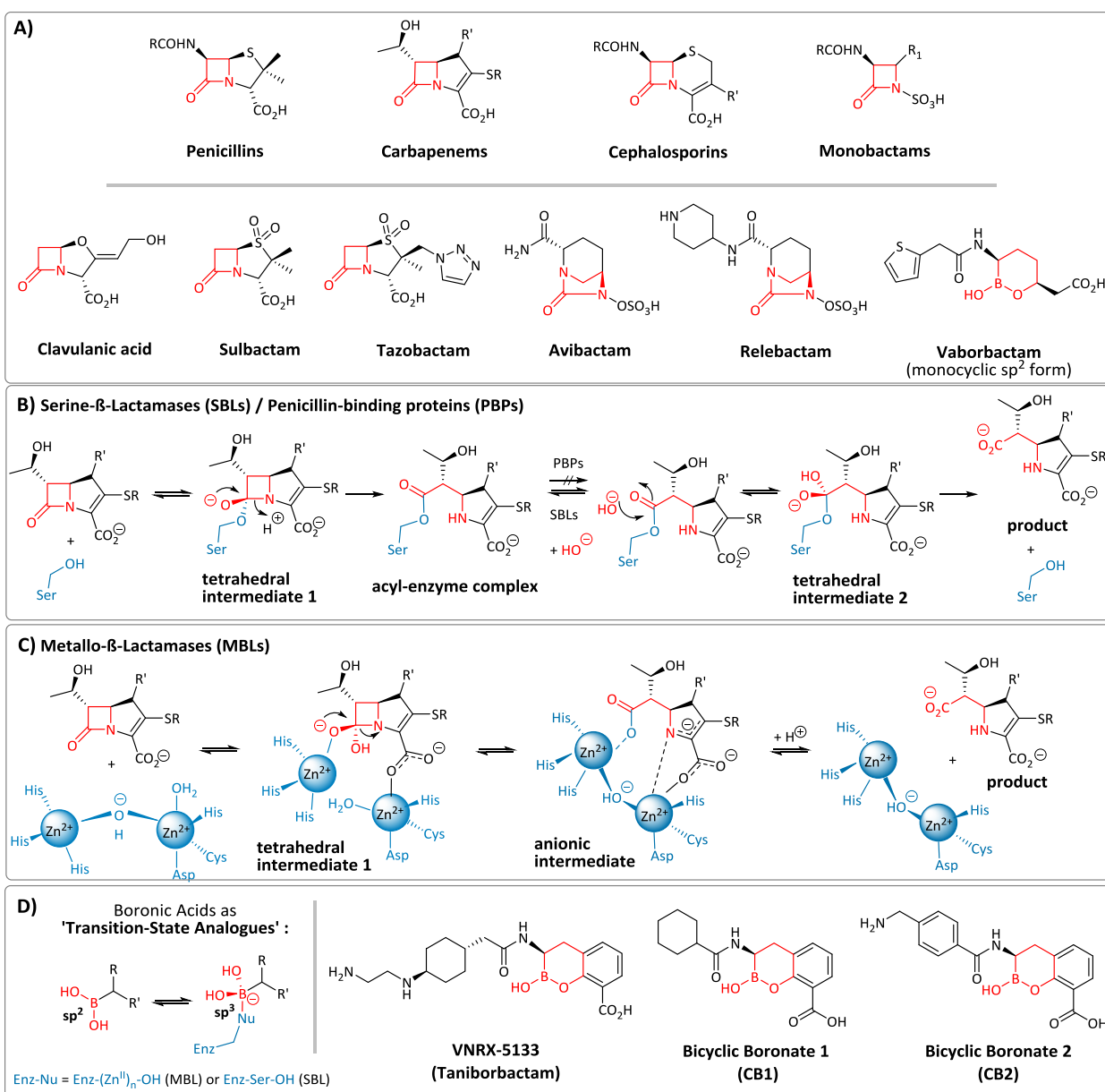
Figure 1. β-Lactam antibacterials, β-lactamase inhibitors in clinical use, outline mechanisms for serine- and metallo-β-lactamase (SBL and MBL) catalysis, and bicyclic boronates in research and development. (A) Major classes of β-lactam antibiotics and SBL inhibitors currently in clinical use, including the clinically approved "monocyclic" boron-containing inhibitor vaborbactam (which has little MBL activity[15]); mode of action of (B) SBLs and (C) MBLs, exemplified by hydrolysis of a carbapenem. Note that the hydrolyzed carbapenem products can be produced in different tautomeric forms. (D) Note that the ability of boronate inhibitors (e.g., VNRX-5133) to interchange between sp² and sp³ forms can enable them to mimic both substrates (sp² carbonyl) and the first tetrahedral intermediate (sp³). Selected examples of bicyclic boronates from research and development are shown.

is evidence that SBLs and MBLs have potential to evolve to hydrolyze it.[14]

There is thus interest in the development of non-acylating inhibitors of β-lactamases and PBPs. With this objective in mind, multiple approaches and compounds have been explored, most with relatively little success. In pioneering work, acyclic boronic acids have been developed as multiple myeloma drugs, targeting human proteasomes, which employ nucleophilic threonine catalysis.[16] After a long gestation period, boronic acids/boronate esters have emerged as β-lactamase inhibitors with considerable clinical potential.[17−20] Boronate-based inhibitors are of mechanistic interest as, in their tetrahedral (sp³-hybridized) forms, they are proposed to be analogues of the high-energy

"tetrahedral" intermediates present in the catalytic cycle of the nucleophilic serine enzymes, such as SBLs (Figure 1B) and PBPs, as well as MBLs (Figure 1C).[21,22] It has also been proposed that boron in its sp²-hybridized form can mimic the β-lactam carbonyl group of substrates, which β-lactamases bind highly efficiently.[23]

Recent work has led to the first clinical introduction of a boronic acid-based SBL inhibitor, vaborbactam (formerly RPX7009), for use in combination with the carbapenem meropenem.[24,25] Whilst the early boronic acid SBL inhibitors are apparently predominantly acyclic in solution, vaborbactam adopts a monocyclic boronate structure, as observed at the active site of an SBL (CTX-M-15).[24] Vaborbactam, however,
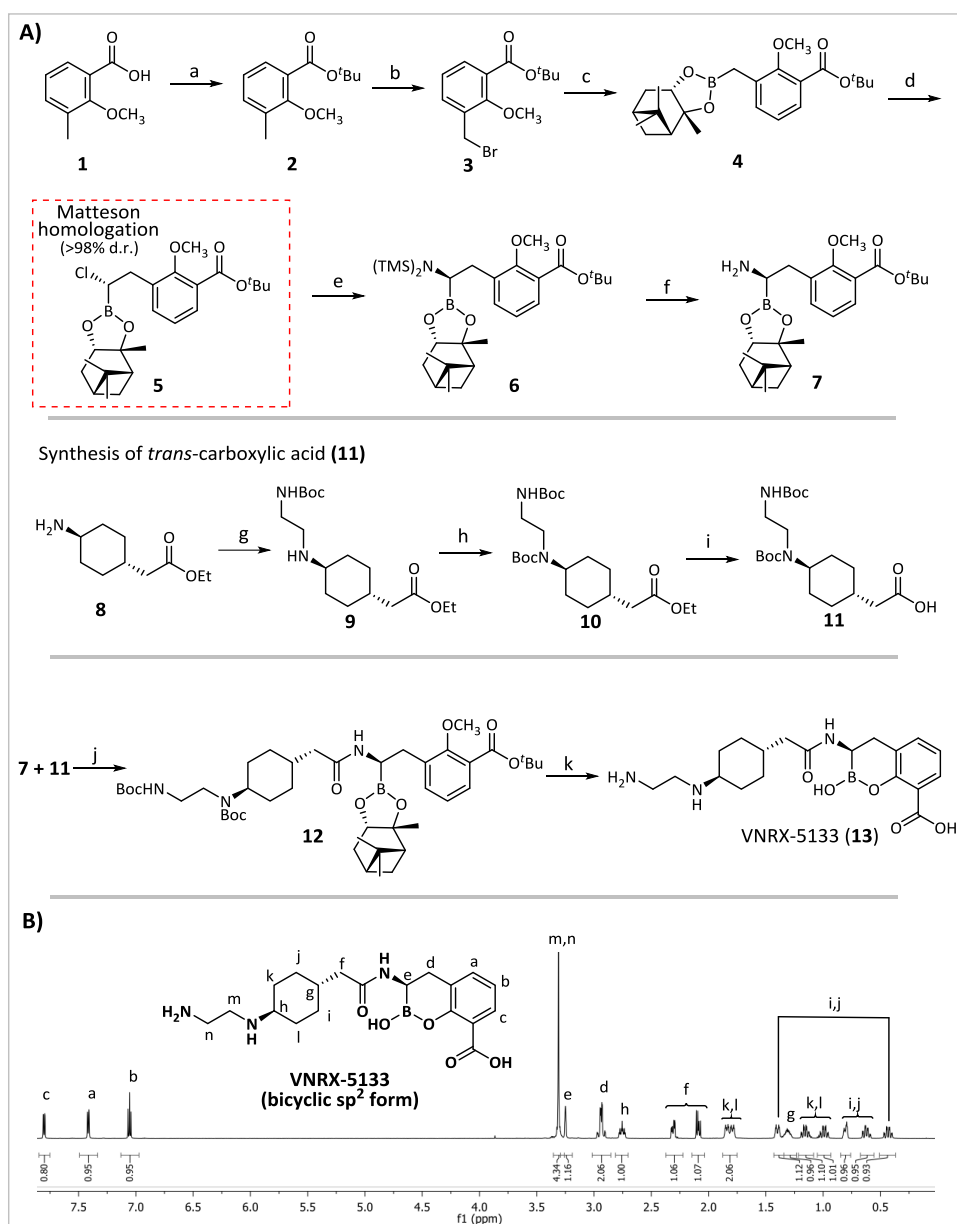
Figure 2. Synthesis and NMR analysis of VNRX-5133. (A) Reagents and conditions: (a) oxalyl chloride, cat. DMF, CH$_2$Cl$_2$, room temperature (rt), 90 min and then 2-methylpropan-2-ol, 40 °C, 18 h; (b) N-bromosuccinimide, benzoyl peroxide, CCl$_4$, reflux, UV, 5 h; (c) bis[(+)-pinanediolato]diboron, Pd(dppf)Cl$_2$, KOAc, 1,4-dioxane, 95 °C, 16 h; (d) CH$_2$Cl$_2$, tetrahydrofuran (THF), n-BuLi, −100 °C, 45 min and then 4 in THF, ZnCl$_2$, −95 °C to rt, overnight; (e) lithium bis(trimethylsilyl)amide, THF, −100 °C to −78 °C, 2 h; (f) MeOH, THF, −10 °C to rt, 1 h; (g) K$_2$CO$_3$, 1:1 CH$_2$Cl$_2$/H$_2$O, rt, 1 h and then 2-(boc-amino)ethyl bromide, benzyltriethylammonium chloride, reflux, 18 h; (h) di-*tert*-butyl dicarbonate, N,N-diisopropylethylamine, reflux, 16 h; (i) LiOH·H$_2$O, 1:2:1 THF/EtOH/H$_2$O, rt, 5 h; (j) 11, triethylamine, PyBOP and then crude 7, rt, 75 min; (k) BCl$_3$, CH$_2$Cl$_2$, −78 °C, 1 h. (B) ^{1}H NMR (600 MHz) of high-performance liquid chromatography (HPLC)-purified VNRX-5133 in D$_2$O.

has limited SBL coverage and only moderately inhibits MBLs.[15,26] By contrast, recent studies have indicated that bicyclic boronates can inhibit a broader range of SBLs and, importantly, some B1 subfamily MBLs.[27,28]

The potential of bicyclic boronates to act as dual action inhibitors of SBLs and MBLs is reported in the academic[27−29] and patent literature.[30] Taniborbactam (VNRX-5133) is now in phase 3 clinical trials as a relatively broad-spectrum β-lactamase inhibitor. However, while its ability to extend the activity of β-lactam antibiotics against SBL- and MBL-harboring bacteria is reported,[31−33] the breadth of its activity versus isolated β-lactamases has been unclear. There are no reported structures of VNRX-5133 complexed with SBLs or MBLs in the PDB

database. To address these issues, we synthesized VNRX-5133 and tested it for inhibition against a panel of SBLs and MBLs. The results support the potential of bicyclic boronates for broad-spectrum β-lactamase inhibition. Together with previous studies, they also illustrate how the ability of boron to readily interchange between different hybridization states and binding modes in water can help to enable potent inhibition.

■ RESULTS AND DISCUSSION

Synthesis. VNRX-5133 was synthesized via a modified version of the reported[30] stereocontrolled route in 11 steps from 2-methoxy-3-methylbenzoic acid **1** via Matteson homologa-tion[34] (Figure 2A).

Table 1. Activities of VNRX-5133 versus representative serine- and metallo-β-lactamases[a]

	class	enzyme	VNRX-5133 IC$_{50}$ (μM)	vaborbactam[15] IC$_{50}$ (μM)	CB2[27,28] IC$_{50}$ (μM)
SBL	A	TEM-116	0.12	6	0.003[27]
MBLs	B1	IMP-1	2.51	126	1[27]
	B1	NDM-1	0.01	631	0.029[27]
	B1	VIM-1	0.0079	398	0.085[28]
	B1	VIM-2	0.0005	316	0.003[27]
	B2	CphA	2.51	631	>100[27]
	B3	L1	>10	336	not inhibited[41]
SBL	C	AmpC (*P. aeruginosa*)	0.301	5	0.12[28]
SBLs	D	OXA-10	0.234	>400	not available
	D	OXA-10[b]	0.645	>400	5.1[28]
	D	OXA-48	0.537	25	not available
	D	OXA-48[b]	2.39	32	2.6[28]

[a]IC$_{50}$ values of VNRX-5133 against a panel of SBLs and MBLs (see Supporting Information Table S1 for error analysis). SBL, serine-β-lactamase; MBL, metallo-β-lactamase. [b]These assays were run in the presence of 100 mM aqueous sodium bicarbonate.

The requisite (+)-pinanediol boronate precursor **4** (87%) was prepared according to reported procedures.[27] Stereoselective one-carbon homologation of **4** using in situ generated dichloromethyllithium[35] gave (*S*)-chloride **5**. Initial yields after chromatographic purification were low. Following optimization, **5** was routinely obtained in improved yield (55−61%) in high diastereomeric purity (d.r., <98%, ^{1}H NMR).[36] Reaction of **5** with lithium bis(trimethylsilyl)amide at −90 °C gave bis(trimethylsilyl)-protected amine **6** with inversion of configuration. To avoid decomposition, crude *N*-**6** was not separated and immediately treated with stoichiometric anhydrous methanol (−10 °C to room temperature, THF) to give amine **7**.

The desired side chain carboxylic acid with the *trans* stereochemistry **11** was prepared from commercial ethyl 2-(*trans*-4-aminocyclohexyl) acetate hydrochloride **8** in three steps. Initial attempts to install the desired ethane-1,2-diamine moiety via *N*-alkylation were unproductive, possibly due to the low solubility of **8** in the tested organic solvents. Biphasic conditions (1:1, CH$_2$Cl$_2$:H$_2$O) employing 5 mol% benzyltriethylammonium chloride as a phase-transfer catalyst gave **9** (49%) following chromatography, which was Boc-protected to give ethyl ester **10** (82%). Saponification followed by ion-exchange chromatography (Amberlite H-120) gave **11** (67%).

The formation of the amide linking **7** and **11** was achieved using (benzotriazole-1-yloxy)tripyrrolidinophosphonium hexafluorophosphate (PyBOP)[37] to give **12** in moderate yield (34%). One-pot cleavage of the Boc, *tert*-butyl, methyl ether protecting groups, and the chiral auxiliary using BCl$_3$ (−78 °C, CH$_2$Cl$_2$) followed by acidic workup (likely aiding the spontaneous bicyclization) gave VNRX-5133 (**13**) (42%) following HPLC purification. VNRX-5133 (**13**) was thus prepared in 3% overall yield over 6 linear steps (excluding steps e and f, Figure 2A, where intermediates were not isolated). The route described here represents an improvement for the asymmetric synthesis of VNRX-5133 compared to that reported,[30] with the number of steps being cut from 16 to 11. There is, however, clear scope for further optimization.

Biochemical Evaluation. We screened VNRX-5133 for activity against a panel of clinically relevant SBLs and MBLs (Table 1) using an established method involving hydrolysis of the "fluorogenic" cephalosporin probe FC5[38] or meropenem for CphA.[27] In conference reports, VNRX-5133 has been reported to inhibit both SBLs and MBLs.[31,33,39] Consistent with this and our previously reported results on the inhibition of all classes of

β-lactamases by structurally related (bi)cyclic boronates,[27−29] VNRX-5133 manifests submicromolar half-maximal inhibitory concentration (IC$_{50}$) values (0.53−0.008 μM) against all major classes of clinically relevant β-lactamases tested, with particularly potent activity, i.e., in the subnanomolar range (IC$_{50} \sim 0.5$ nM), against the Verona-integron-encoded MBL-2, VIM-2. Notably, VNRX-5133 was less active against the clinically important imipenemase (IMP)-1 B1 MBL (IC$_{50} \sim 2.51$ μM) and the B2 MBL from *Aeromonas hydrophila* CphA (CphA, IC$_{50} \sim 2.51$ μM), nor did it inhibit subclass B3 MBL L1 from *Stenotrophomonas maltophilia*. The comparison of IC$_{50}$ values reveals that VNRX-5133 (taniborbactam) is 50 to >50 000-fold more potent against the clinically relevant MBLs compared to vaborbactam[15] (VNRX-5133 is, in general, more potent than the structurally related bicyclic boronate CB2[26,27] against the same enzymes). Variation in the pre-incubation times of VNRX-5133 with subclass B1 MBL NDM-1 did not result in different IC$_{50}$ values (Supporting Information Table S2 and Figure S33), thus supporting the case for the reversible inhibition by VNRX-5133, as observed for related bicyclic boronate inhibitors.[29,40]

Notably, improved inhibition with respect to vaborbactam is also observed for VNRX-5133 against the class A narrow-spectrum β-lactamase TEM-116 (500-fold increase) and for the tested class D SBLs (a 10- to 2000-fold increase, Table 1). In particular, VNRX-5133 manifests moderate inhibition of the narrow-spectrum oxacillinase OXA-10 (IC$_{50} \sim 0.234$ μM), which is not inhibited by vaborbactam (Table 1). Only moderate inhibition of the OXA-48 carbapenemase was observed (IC$_{50} \sim 0.537$ μM). Overall, these results support the proposal that VNRX-5133 possesses an unusually broad-spectrum inhibitory activity against Ambler Class A (ESBLs), B (NDM and VIM), C (AmpC from *P. aeruginosa*) and, to a somewhat lesser extent, D (OXA) β-lactamases. Nonetheless, the lower activity of VNRX-5133, in particular, against the subclass B1 MBL IMP-1, as well as the tested B2/B3 MBLs implies that there is scope for further optimization of this new inhibitor class.

Crystallography. To investigate the binding mode of VNRX-5133 to β-lactamases, we initiated crystallographic analyses and obtained structures of it in complex with the class D SBL OXA-10 and the B1 subclass MBL NDM-1, at resolutions of 2.17 Å (space group: P2$_1$2$_1$2$_1$) and 1.51 Å (space group: P2$_1$2$_1$2$_1$), respectively. In each structure, there are two chains (A/B) in the asymmetric unit.
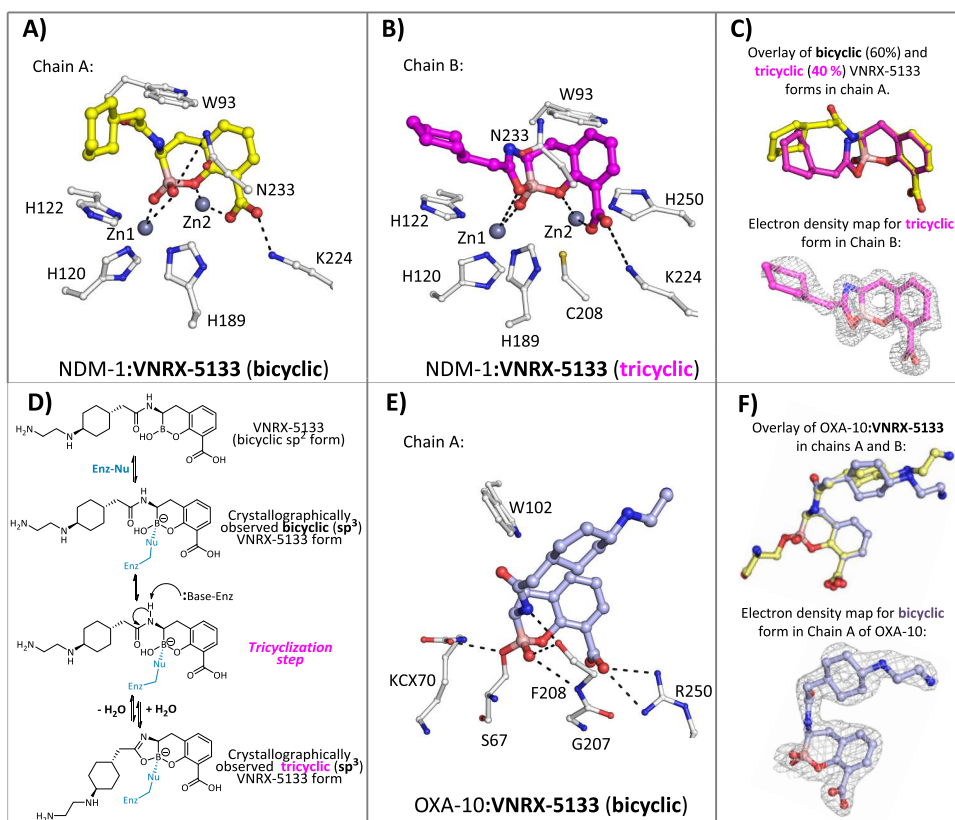
Figure 3. Structural basis of serine- and metallo-β-lactamase inhibition by VNRX-5133. (A) View from a crystal structure of VNRX-5133 complexed with NDM-1 (PDB ID: 6RMF) in chain A showing the major observed bicyclic form (yellow). (B) View from a crystal structure of VNRX-5133 complexed with NDM-1 (PDB ID: 6RMF) in chain B showing the tricyclic form (magenta). (C) An overlay of bicyclic (60%, yellow) and tricyclic (40%, magenta) forms of VNRX-5133 in chains A or B of NDM-1 and 2mFo-DFc electron density for the tricyclic inhibitor form in chain B (contoured to 3σ, gray mesh). (D) Proposed mechanism for formation of the unexpected tricyclic VNRX-5133 complex. Enz-Nu = Enz-(ZnII)$_n$-OH (MBL) or Enz-Ser-OH (SBL). (E) Binding mode of VNRX-5133 to the OXA-10 SBL (PDB ID: 6RTN). (F) Comparison of the binding modes of VNRX-5133 in complex with OXA-10 (PDB ID: 6RTN) in chain A (pale blue) and chain B (pale yellow); omit electron density for the bicyclic form in chain A (contoured at 3σ, gray mesh).

After soaking of an NDM-1 crystal with VNRX-5133, there was clear $F_o - F_c$ density corresponding to bound VNRX-5133 in the active site in both chains A and B. Unexpectedly, the electron density (Figure 3) indicated the presence of a tricyclic form of VNRX-5133 (Figure 3B, and Supporting Information Figure S2A), which was refined at full occupancy in chain B (with an average B-factor of 18.02 Å^2). In chain A, a mixture of both the bicyclic (as solely observed with OXA-10) (Figure 3A) and tricyclic forms was modeled (at occupancies of 0.6 and 0.4, respectively). The ethylamino atoms of the VNRX-5133 side chain in both chains A and B lacked observable electron density and were removed in the final model. The tricyclic structure is probably formed by cyclization of the side chain amide oxygen onto the boron. Although there is no obvious basic amino acid residue close enough to the side chain amide to catalyze this reaction manifested in the crystal structure, this type of reaction has precedent in synthetic chemistry.[42]

For both bicyclic and tricyclic forms with NDM-1, the bicyclic "boronate core", including the aryl carboxylate, adopts nearly identical binding modes (Figure 3C). Notably, binding of VNRX-5133 to NDM-1 increases the Zn1–Zn2 distance from ~3.6 Å (e.g., PDB ID: 5ZGZ[43]) to 4.3 Å (in both chains A and B); a similar increase has been observed on binding/reaction of the antibiotic ampicillin with NDM-1 (PDB ID: 5ZGE[43]) and on binding of CB2 to VIM-2.[43] Such changes in the positioning

of metal ions induced by inhibitor–substrate interactions in β-lactamase catalysis have also been observed with extended X-ray absorption fine structure (EXFAS) spectroscopy studies, as shown in the case of the subclass B3 MBL L1 from *S. maltophilia*[44] and with other metallo-enzymes (see e.g.,[45−47]); it may also be that the extent of such metal ion translocations is not fully reflected in crystallographic compared to solution studies. It should also be noted that the precipitants used in crystallography experiments for NDM-1:**VNRX-5133** and OXA-10:**VNRX-5133** structures were at pH 5.8 and pH 8.0, respectively.

One boron-bound oxygen effectively bridges the two active site zinc ions in NDM-1 but is closer to Zn1 (1.9 Å) than Zn2 (3 Å). The boron-bound oxygen that "becomes" part of the 5-membered ring of the tricyclic VNRX-5133 (Figure 3B) is positioned to make a significantly weaker interaction with Zn2 (2.8 Å) than Zn1 and is positioned almost identically to the same boron-bound oxygen in the bicyclic VNRX-5133 structure (Figure 3C). For comparison, CB2 binding to VIM-2 results in interactions of the boron-bound oxygens of 2.6 and 1.9 Å to Zn2.[27] A number of other interactions of VNRX-5133 are conserved with respect to other bicyclic boronates (i.e., CB2 and others[27−29]), including that of the aryl carboxylate with Zn2 and Lys$_{224}$ and the "endocyclic" boronate ester oxygen with Zn2. The L3 loop, which is proposed to be involved in binding
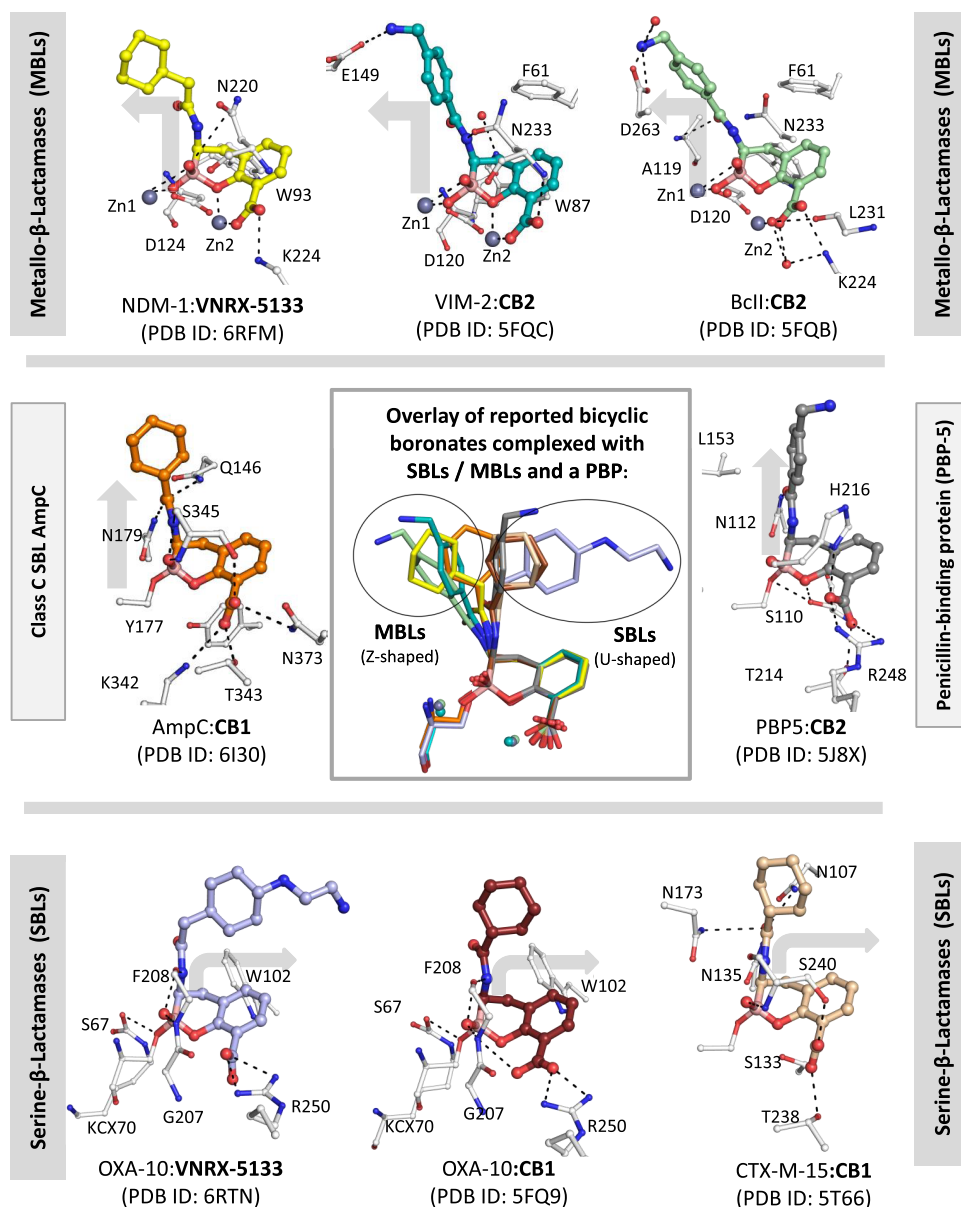
Figure 4. Overlays of reported bicyclic boronate structures and VNRX-5133 in MBLs, SBLs, and a PBP reveal different side-chain orientations. Views from NDM-1:VNRX-5133 (yellow, bicyclic form, PDB ID: 6RFM), VIM-2:CB2 (teal, PDB ID: 5FQC[27]), BcII:CB2 (pale green, PDB ID: 5FQB[27]), AmpC:CB1 (orange, PDB ID: 6I30[29]), PBP-2:CB2 (gray, PDB ID: 5J8X[27]), OXA-10:VNRX-5133 (pale blue, PDB ID: 6RTN), OXA-10:CB1 (brown, PDB ID: 5FQ9[27]), and CTX-M-15:CB1 (wheat, PDB ID: 5T66[28]). Note that although the crystallographically observed orientations of the acylamino side chains vary, the binding modes of cyclic ring systems and their carboxylate are conserved, including for VNRX-5133. The acylamino side chains adopt two broad orientations, reflecting binding to SBLs (U-shaped). The VNRX-5133 acylamino side chain adopts clearly different conformations in the bicyclic inhibitor forms in both OXA-10 and NDM-1 structures (Figure 4). Although care should be taken in assuming that the crystallographically observed binding modes accurately reflect the solution behavior, the structural observations imply that the optimized VNRX-5133 side chain can enable potent inhibition of different β-lactamase classes, by adopting different binding modes. Structural analyses of the cyclic boronates bound to MBLs and SBLs reveal that the acylamino side chain adopts two types of orientations (at least in the crystalline state), reflecting binding to SBLs or MBLs. These observations imply that there is likely further scope for side chain optimization, including with respect to extending the scope and potency of MBL inhibition and obtaining more potent (bi/tri)cyclic boronate-based PBP inhibitors. Importantly, comparison of the OXA-10 and NDM-1 structures with those observed for other structurally related compounds, i.e., CB1/CB2 (which differ from VNRX-5133 only in their C-3 acylamino side chains) when complexed with SBLs (OXA-10,[27] CTX-M-15,[28] AmpC[29]), MBLs (NDM-1,[27] VIM-2,[27] BcII[27]), and a PBP (PBP-5[27]), reveal conservation in the binding mode of the bicyclic boronate core (Figure 4). Even allowing for the observed tricycle formation with NDM-1, similar conformations are observed across all Ambler classes of β-lactamases as well as with a PBP (Figure 4). Superimposition of structures of OXA-10:**VNRX-5133** and NDM-1:**VNRX-5133** with analogous structures of the respective enzymes with "intermediate" complexes derived from substrates (e.g., hydrolyzed benzylpenicillin) reveals the binding modes adopted by VNRX-5133/related inhibitors overlap with those adopted by hydrolyzed β-lactams (Supporting Information Figures S1 and S2B).

inhibitors/substrates,[48] is partly disordered in the case of the VNRX-5133 complex (residues 67−70 and 68−70 could not be modeled in chains A and B, respectively) and has high B-factors

compared to the rest of the main chain, indicating flexibility.

These observations suggest that the L3 loop may not have an

important role in stabilizing VNRX-5133 NDM-1 binding (Supporting Information Figure S4).

The tricyclic form observed in NDM-1 is probably generated by the reaction of the acylamino side-chain carbonyl group with the VNRX-5133 boron, together with associated loss of water/hydroxide (Figure 3D). Given that we observed evidence for both the bicyclic and tricyclic forms in the crystal structure (Figure 3A,B), it seems likely that tricyclization occurs at the active site, though we cannot rule out the presence of the tricyclic form at low concentrations in the solution phase.[42] Further studies will be necessary to exclude the possibility that the observed tricyclic inhibitor form is not a crystallization artifact; it has been proposed that at least one MBL−inhibitor complex crystal structure, i.e. the mono-zinc carbapenemase MBL CphA in complex with biapenem, does not necessarily reflect the catalytic pathway in solution.[49,50] Nevertheless, the observation of a tricycle is a striking example of the ability of boron-based inhibitors to interchange between different forms, potentially giving a tightly bound enzyme−inhibitor complex.

In the case of the OXA-10:**VNRX-5133** complex structure (Figure 3E), the inhibitor is observed to bind similarly in chains A and B (Figure 3F), with the boron atom covalently linked to the nucleophilic serine (Ser_{67}), likely mimicking the tetrahedral intermediate in SBL/MBL catalysis (Figure 1B,C).[27,28] The essential conserved lysine (Lys_{70}),[51] which acts as a general acid/base, is, at least predominantly, in its carbamylated (KCX_{70}) form in both chains A and B (Supporting Information Figure S3). Comparison of this structure with that of OXA-10 complexed with the structurally related bicyclic boronate inhibitor CB1 (PDB ID: 5FQ9[27]) reveals that, while the bicyclic cores of both inhibitors manifest similar binding modes, there are substantial variations in the conformations adopted by their acylamino side chains, which have implications for the side chain optimization (Figure 4). The boron-containing bicyclic cores and the acylamino side chains of both VNRX-5133 and CB1 are positioned to make hydrophobic/aromatic interactions with Tyr_{102} and Met_{99}. Although there is some variation in their precise conformations, the VNRX-5133 and CB1 aryl carboxylates are both positioned to make polar interactions with Gly_{207} and Arg_{250} that bind the analogous carboxylates in β-lactams (Supporting Information Figure S1). Note that some variations of the aryl carboxylate binding modes are anticipated, given the differences in the precise modes of carboxylate binding employed by different classes of SBL/MBL/PBP.

Microbiology. Antimicrobial susceptibility testing of VNRX-5133 in combination with meropenem (carbapenem) or cefepime (cephalosporin) was performed in minimal inhibitory concentration (MIC) antimicrobial assay format utilizing six clinical isolates of NDM-1-producing clinically relevant strains of *Escherichia coli* and *Klebsiella pneumoniae* (Table 2). In all cases, the MIC values of cefepime/meropenem were significantly reduced in the presence of VNRX-5133 compared to those in its absence (MIC > 64 μg mL^{-1}). Both cefepime/VNRX-5133 and meropenem/VNRX-5133 combinations were highly active against all six of the NDM-1-producing clinical isolates tested, with MIC ranges of 16−0.25 and 1−0.125 μg mL^{-1}, respectively. These results reveal the potential of VNRX-5133 to act against clinically relevant MBLs (i.e., NDM-1) in bacteria, consistent with the results from clinical trials with VNRX-5133.[44,45]

Table 2. Effect of VNRX-5133 on Cefepime/Meropenem MICs for Selected NDM-1 MBL-expressing *Enterobacteriaceae*[a]

strain	species	genotype	Cef/MEM MIC (μg mL^{-1})	Cef/MEM + VNRX-5133 (10 μg mL^{-1})
S117	Ec	NDM-1	>64	16/1
IR57	Ec	NDM-1	>64	8/0.5
B64	Kp	NDM-1	>64	0.25/0.25
B68-1	Kp	NDM-1	>64	0.5/0.5
IR43	Kp	NDM-1	>64	0.5/0.25
91N	Ec	NDM-1	>64	4/0.125

[a]Ec, *Escherichia coli*; Kp, *Klebsiella pneumoniae*; MEM, meropenem; Cef, cefepime.

CONCLUSIONS

The overall results clearly support the clinical potential[39,52−54] of VNRX-5133 (taniborbactam) for inhibition of MBLs as well as SBLs, thus potentially extending the current utility of current β-lactam antibiotics. In this regard, VNRX-5133 is different to the clinically approved boron-containing β-lactamase inhibitor vaborbactam, which has little activity versus clinically relevant MBLs.[15,26] The coverage of clinically relevant MBLs (and SBLs) by VNRX-5133, however, is imperfect, with significantly lower or no inhibition being observed for clinically relevant IMP-1, L1, or OXA-48 (Table 1). There is thus scope for further optimization of this promising new class of β-lactamase inhibitors.

The crystallographic results also further imply the potentially unique properties of boron-containing small molecules to interchange between different binding modes/hybridization states, thus potentially enabling (more) potent inhibition. It is possible that bicyclic boronates can bind to SBLs and MBLs in their sp^2 hybridization state, which mimics that of the β-lactam.[23] Once bound at the active site, they can then react with the SBL nucleophilic serine or MBL-Zn(II)-bridged water/hydroxide to give a tightly bound sp^3 complex, mimicking the tetrahedral intermediate in catalysis. Note that with the MBLs, in principle, the sp^3 boronate form could bind to the active site, with a displacement of the "hydrolytic" water/hydroxide from the active site Zn(II) ions.[27−29]

The potential of boron to enable further reaction when an inhibitor is bound to a protein is strikingly evidenced by the crystallographic observation of the tricyclic form in the case of NDM-1 (Figure 3B). Further biophysical analyses are required to demonstrate relevance of the tricyclic inhibitor form in solution and thus rule out the possibility that the tricyclic inhibitor form is an artifact arising from the crystallization conditions. This ability has been exploited in the case of boron compounds in dynamic combinatorial chemistry[55] and is manifested in the reaction of amidomethylboronic acid inhibitors with two active site serines in the case of penicillin-binding protein from *Actinomadura* sp. R39.[56] We propose that the ability of boron compounds to "morph" between states can be further exploited in inhibitor/modulator design, especially where conformational changes during ligand binding are desirable. Such applications will likely require a combination of precise activity/binding assays coupled with detailed biophysical studies.

EXPERIMENTAL SECTION

General Procedures. Unless otherwise stated, reactions were performed under argon using dried glassware and solvents. All

commercially available chemicals, reagents, and solvents were used as commercially supplied or purified using appropriate standard procedures. Petroleum ether (PetEt) refers to distilled light petroleum of fraction 30−40 °C. A cold bath at −100 °C was prepared by addition of liquid nitrogen to a mixture of 1:1 ethanol/methanol. Reactions were monitored by thin layer chromatography (TLC) using Merck silica gel 60 F$_{254}$ aluminum sheets, 5 × 7.5 cm, and using an liquid chromatography−mass spectrometry (LC−MS) system (Agilent Technologies 1260 Infinity Series) fitted with a 6120 Quadrupole mass spectrometer and a Merck Chromolith Performance C18 (100 × 4.2 mm) HPLC column. TLC analyses were visualized by exposure to UV irradiation (λ_{max} = 254 or 365 nm) and by dipping the plates in phosphomolybdic acid, potassium permanganate, or ninhydrin followed by heating with a heat gun. Chromatographic purifications were performed using a Biotage Isolera flash purification system with Biotage prepacked SNAP KP-Sil or SNAP-ULTRA columns and analytical-grade solvents. ^{1}H, ^{13}C, and ^{11}B NMR spectra were recorded using Bruker AVIII HD 400, AVIII HD 500, or AVIII 600 instruments in the solvents indicated. Deuterated solvents were used as supplied. Chemical shifts (δ), referenced using residual solvent peaks, are reported in parts per million downfield from tetramethylsilane or residual solvent peak as internal standard. Multiplicity is given as s (singlet), d (doublet), t (triplet), q (quartet), m (multiplet), br (broad), app (apparent), or a combination of these. Coupling constants, J, are reported in hertz (Hz) to the nearest 0.5 Hz. COSY, HSQC, and/or HMBC spectra were utilized to aid the chemical shift assignments where appropriate. Infrared (IR) spectra were recorded using a Bruker Tensor 27 FT-IR spectrometer; wavenumbers (ν_{max}) are quoted in cm^{-1}. Analytical-grade solvents and a PerkinElmer 341 polarimeter were used for measurement of optical rotations; $[\alpha]_D^T$ values are reported in 10^{-1} deg cm^2 g^{-1}, and concentrations (c) are quoted in g per 100 mL; D refers to the D-line of sodium (589 nm), and temperatures (T) are given in degrees Celsius (°C). Preparative HPLC was run using a Shimadzu prep-LC system equipped with an ACE 5 μm C18 column (100 mm × 21.2 mm id). HPLC preparatory method A refers to [binary gradient: 10 mM HCl in water (solvent A), acetonitrile + 25% MeOH (solvent B), 15 mL min^{-1}] 0−5 min gradient 1% B; 5−30 min gradient 10% B; 31−36 min gradient 90% B, 37−45 min gradient 1% B; UV detection at 254 nm. Low-resolution mass spectra were recorded using an Agilent 6120 Quadrupole MS instrument. High-resolution mass spectra (HRMS) were recorded using a Bruker MicroTOF instrument with an ESI source and time-of-flight (TOF) analyzer. The LC−MS system (Agilent Technologies 1260 Infinity Series) was fitted with a 6120 Quadrupole mass spectrometer and a Merck Chromolith Performance C18 (100 × 4.2 mm) HPLC column. All compounds synthesized were ≥95% pure as judged by ^{1}H and ^{13}C NMR, LC−MS, or qHNMR analyses.

tert-Butyl 2-Methoxy-3-methylbenzoate (**2**). To a solution of 2-methoxy-3-methylbenzoic acid **1** (2 g, 12.0 mmol, 1 equiv) and anhydrous *N,N*-dimethylformamide (5 drops) in anhydrous CH$_2$Cl$_2$ (20 mL) was added oxalyl chloride (1.54 mL, 17.9 mmol, 1.5 equiv) dropwise under Shlenk conditions. The resultant mixture was stirred at room temperature (rt) for 90 min, before volatiles were removed in vacuo. The resulting oil was dissolved in anhydrous 2-methylpropan-2-ol (30 mL) and stirred at 40 °C for 18 h before the volatiles were removed in vacuo. H$_2$O (30 mL) and CH$_2$Cl$_2$ (60 mL) were added, and the layers were separated. The aqueous layer was extracted with CH$_2$Cl$_2$ (2 × 60 mL). The combined organic layers were washed with brine (30 mL), dried (MgSO$_4$), and then concentrated in vacuo. The crude material was purified by flash chromatography (0−30% EtOAc in cyclohexane) to afford the desired product **2** as a colorless oil (1.70 g, 63%). R_f 0.50 (19:1 CH$_2$Cl$_2$−MeOH); ^{1}H NMR (600 MHz, CDCl$_3$) δ 7.52−7.42 (m, 1H, H-4), 7.25−7.20 (m, 1H, H-2), 6.95 (app t, J = 7.5 Hz, 1H, H-3), 3.75 (s, 3H, H-16), 2.24 (s, 3H, H-9), 1.53 (s, 9H, C(CH$_3$)$_3$); ^{13}C NMR (101 MHz, CDCl$_3$) δ 166.1 (C-8), 158.0 (C-6), 134.5 (C-2), 132.6 (C-1), 129.0 (C-4), 126.9 (C-5), 123.5 (C-3), 81.4 (C-12), 61.5 (C-16), 28.4 (C(CH$_3$)$_3$), 16.2 (C-9); ν_{max}/cm (neat): 2978, 2360, 1720, 1593, 1468, 1416, 1367, 1169; HRMS (ESI-TOF) calcd for C$_{13}$H$_{18}$O$_3$^{23}Na [M + Na]$^+$: 245.11482, found: 245.11487.

tert-Butyl 3-(bromomethyl)-2-methoxybenzoate (**3**). A mixture of *tert*-butyl 2-methoxy-3-methylbenzoate **2** (1.69 g, 7.60 mmol, 1 equiv), *N*-bromosuccinimide (NBS; 1555 mg, 8.74 mmol, 1.15 equiv), and benzoyl peroxide (368 mg, 1.52 mmol, 0.2 equiv) in CCl$_4$ (20 mL) was refluxed in the presence of a Philips HB175 (75 W, UV type 3) lamp for 5 h. The reaction mixture was then cooled to rt, the precipitate was removed by filtration, and the filtrate was concentrated in vacuo. The crude material was purified by flash chromatography (0−25% petroleum ether (PetEt) in cyclohexane) to afford the desired product **3** as a colorless oil (1.33 g, 58%). R_f 0.50 (19:1 CH$_2$Cl$_2$−MeOH); ^{1}H NMR (400 MHz, CDCl$_3$) δ 7.66−7.60 (m, 1H, H-4), 7.48−7.41 (m, 1H, H-2), 7.04 (app t, J = 8.0 Hz, 1H, H-3), 4.52 (s, 2H, H-9), 3.90 (s, 3H, H-16), 1.54 (s, 9H, C(CH$_3$)$_3$); ^{13}C NMR (151 MHz, CDCl$_3$) δ 165.3 (C=O), 158.2 (C-6), 134.6 (C-2), 132.3 (C-1), 132.2 (C-4), 127.0 (C-5), 123.9 (C-3), 81.9 (C(CH$_3$)$_3$), 62.9 (C-16), 28.3 (C(CH$_3$)$_3$), 27.8 (C-9); ν_{max}/cm (neat): 2979, 2360, 1718, 1591, 1469, 1423, 1080; HRMS (ESI-TOF) calcd for C$_{13}$H$_{17}$O$_3$^{79}Br^{23}Na [M + Na]$^+$: 323.02533, found: 323.02542.

tert-Butyl 2-Methoxy-3-(((3aR,4R,6R,7aS)-3a,5,5-trimethylhexahydro-4,6-methanobenzo[d][1,3,2]dioxaborol-2-yl)methyl)-benzoate (**4**). *tert*-Butyl 3-(bromomethyl)-2-methoxybenzoate **3** (1.7 g, 5.64 mmol, 1 equiv), bis[(+)-pinanediolato] diboron (2.43 g, 6.80 mmol, 1.2 equiv), and potassium acetate (1108 mg, 98.1 mmol, 2 equiv) were suspended in anhydrous 1,4-dioxane (22.5 mL). The vessel was degassed for 20 min, and then Pd(dppf)Cl$_2$ (228 mg, 0.28 mmol, 5 mol%) was added. The reaction mixture was refluxed at 95 °C for 16 h and then concentrated in vacuo. The residue was redissolved in EtOAc (20 mL) and filtered through a Celite pad. The filtrate was concentrated to dryness under reduced pressure, and the crude material was purified by flash chromatography (0−20% EtOAc in cyclohexane) to afford the desired product as a colorless oil (1.79 g, 87%). R_f 0.70 (15:1 PetEt−EtOAc); ^{1}H NMR (400 MHz, CDCl$_3$) δ 7.48−7.42 (m, 1H, H-4), 7.28−7.22 (m, 1H, H-6), 6.94 (app t, J = 7.5 Hz, 1H, H-5), 4.20 (dd, J = 9.0, 2.0 Hz, 1H, H-13), 3.74 (s, 3H, H-29), 2.25 (s, 2H, H-24), 2.24−2.17 (m, 1H, H-15″), 2.13−2.10 (m, 1H, H-12), 1.96 (t, J = 5.5 Hz, 1H, H-16), 1.84−1.80 (m, 1H, H-15′), 1.77−1.74 (m, 1H, H-11″), 1.52 (s, 9H, C(CH$_3$)$_3$), 1.32 (s, 3H, H-23), 1.21 (s, 3H, H-18), 1.12 (d, J = 10.0 Hz, 1H, H-11′), 0.76 (s, 3H, H-19); ^{13}C NMR (101 MHz, CDCl$_3$) δ 166.2 (C-8), 157.5 (C-2), 134.4 (C-6), 134.1 (C-3), 128.6 (C-4), 126.5 (C-1), 123.5 (C-5), 86.0 (C-13), 81.2 (C(CH$_3$)$_3$), 78.0 (C-14), 61.6 (C-29), 51.4 (C-15), 39.7 (C-12), 39.6 (C-16), 38.3 (C-17), 35.6 (C-24), 28.7 (C-19), 28.4 (C(CH$_3$)$_3$), 27.2 (C-23), 26.5 (C-11), 24.2 (C-18); ^{11}B NMR (128 MHz, CDCl$_3$) δ 32.8; ν_{max}/cm (neat): 2977, 2918, 2360, 2341, 1721, 1466, 1425. 1367, 1338, 1305, 1279, 1230, 1077, 1028; HRMS (ESI-TOF) calcd for C$_{23}$H$_{33}$O$_5$ ^{10}B ^{23}Na [M + Na]$^+$: 422.23496, found: 422.23471; $[\alpha]_D^{25}$ = +15.0° (c 0.8, CHCl$_3$).

tert-Butyl 3-((S)-2-chloro-2-((3aR,4R,6R,7aS)-3a,5,5-trimethyl-hexahydro-4,6-methanobenzo[d][1,3,2]dioxaborol-2-yl)ethyl)-2-methoxybenzoate (**5**). In an oven-dried three-necked round-bottom flask under an argon flow, a solution of anhydrous CH$_2$Cl$_2$ (0.29 mL, 4.56 mmol, 2.5 equiv) in anhydrous THF (5.5 mL) was cooled to −100 °C. While maintaining a low temperature, *n*-butyllithium (2.5 M in hexanes, 1.16 mL, 1.6 equiv) was added slowly dropwise down the inside wall of the flask (maintaining the temperature below −90 °C at all times). The resulting turbid white suspension obtained by the formation of microcrystalline dichloromethyllithium was stirred at −100 °C for 45 min. Batches that turned black in the above process (signaling the decomposition of dichloromethyllithium) were immediately quenched with isopropanol and water and discarded. A precooled (−90 °C) solution of boronic ester **4** (730 mg, 1.82 mmol, 1 equiv) in anhydrous THF (1.2 mL) was then added dropwise at −95 °C. The resulting bright yellow solution was stirred for 20 min at −95 °C, before the freshly prepared anhydrous ZnCl$_2$ solution (0.7 M in THF, 1.48 mL, 0.8 equiv) was added in one portion. The reaction mixture was then allowed to warm up slowly to rt overnight without removal of the cooling bath. The resultant solution was cooled using an ice bath, quenched with sat. aq NH$_4$Cl solution (20 mL), extracted with EtOAc (3 × 20 mL), washed with brine (15 mL), dried (Na$_2$SO$_4$), filtered, and then concentrated in vacuo. The crude material was purified by flash chromatography (5−50% PetEt in pentane) to afford

the desired product **5** as a pale yellow oil (500 mg, 61%). R_f 0.55 (20:1 PetEt−EtOAc); ^{1}H NMR (500 MHz, CDCl$_3$) δ 7.62 (dd, J = 7.5, 2.0 Hz, 1H, H-4), 7.39 (dd, J = 7.5, 2.0 Hz, 1H, H-6), 7.05 (app t, J = 7.5 Hz, 1H, H-5), 4.35 (dd, J = 9.0, 2.0 Hz, 1H, H-13), 3.85 (s, 3H, H-29), 3.75−3.70 (m, 1H, H-22), 2.26 (dd, J = 14.0, 7.5 Hz, 2H, H-24), 2.25−2.17 (m, 1H, H-15″), 2.10 (m, 1H, H-12), 1.94−1.90 (m, 1H, H-16), 1.84-1.80 (m, 1H, H-15′), 1.78−1.74 (m, 1H, H-11″), 1.45 (s, 9H, C(CH$_3$)$_3$), 1.27 (s, 3H, H-23), 1.22 (s, 3H, H-18) 1.19 (d, J = 10.0 Hz, 1H, H-11′), 0.83 (s, 3H, H-19); ^{13}C NMR (126 MHz, CDCl$_3$) δ 166.2 (C-8), 157.8 (C-2), 137.0 (C-6), 134.4 (C-3), 128.6 (C-4), 125.5 (C-1), 123.5 (C-5), 86.0 (C-13), 81.2 (C-25), 78.0 (C-14), 61.6 (C-29), 51.3 (C-15), 39.6 (C-16), 39.2 (C-17), 35.6 (C-24), 28.7 (C-19), 28.3 (C(CH$_3$)$_3$), 27.2 (C-23), 26.5 (C-11), 24.1 (C-18), C-22 not observed due to peak broadening; ν_{max}/cm (neat): 2979, 2929, 2359, 2341, 1719, 1466, 1421, 1369, 1303, 1254, 1172, 1135, 767; HRMS (ESI-TOF) calcd for C$_{24}$H$_{34}$O$_5$^{10}B^{35}Cl^{23}Na [M + Na]$^+$: 470.21164, found: 470.21167; $[\alpha]_D^{25}$ = −10.0 ° (c 7.6, CHCl$_3$).

tert-Butyl 3-((R)-2-amino-2-((3aR,4R,6R,7aS)-3a,5,5-trimethyl-hexahydro-4,6-methanobenzo[d][1,3,2]dioxaborol-2-yl)ethyl)-2-methoxybenzoate (7). To a stirred solution of (S)-chloride **5** (400 mg, 0.89 mmol, 1 equiv) in anhydrous THF (4 mL) under an argon flow was added a solution of lithium bis(trimethylsilyl)amide (LiHDMS, 1 M in THF, 0.94 mL, 0.94 mmol, 1.05 equiv) dropwise over 30 min at −100 °C. The resultant mixture was stirred at −78 °C for 2 h before the volatiles were removed in vacuo. The resultant thick brown oil was immediately used in the next step without further purification. To a solution of crude bis-TMS-protected amine **6** (500 mg, 0.87 mmol, 1 equiv) in THF (4 mL) was added anhydrous MeOH (2 mL) dropwise at −10 °C. The resultant cloudy solution was stirred at rt for 60 min before the volatiles were removed in vacuo. The crude amine **7** thus obtained as a pale yellow oil was immediately used in the next step without further purification.

Ethyl 2-(trans-4-((2-((tert-butoxycarbonyl)amino)ethyl)-amino)-cyclohexyl)acetate (9). Ethyl-2-(*trans*-4-aminocyclohexyl)acetate hydrochloride **8** (2 g, 9.04 mmol, 1 equiv) was dissolved in 1:1 CH$_2$Cl$_2$-H$_2$O (70 mL), and K$_2$CO$_3$ (2740 mg, 20.7 mmoL, 2.3 equiv) was added. The resultant biphasic suspension was vigorously stirred at rt for 60 min, before benzyltriethylammonium chloride (103 mg, 0.45 mmol, 5 mol%) and 2-(Boc-amino)ethyl bromide (2100 mg, 9.37 mmol, 1.04 equiv) were added in one portion. The reaction mixture was refluxed for 18 h, before it was poured into sat. aq NH$_4$Cl (70 mL). The layers were separated, and the aqueous layer was extracted with CH$_2$Cl$_2$ (3 × 70 mL). The combined organic layers were washed with brine (70 mL), dried (MgSO$_4$), then concentrated in vacuo. The crude material was purified by flash chromatography (0−20% MeOH in CH$_2$Cl$_2$) to afford the desired product **9** as a white solid (1.45 g, 49%). R_f 0.80 (1:1 EtOAc−pentane); mp 118−120 °C; ^{1}H NMR (600 MHz, CDCl$_3$) δ 5.00 (br s, 1H, Boc-NH), 4.05 (q, J = 7.0 Hz, 2H, -OCH$_2$CH$_3$), 3.18−3.04 (m, 2H, CH$_2$), 2.74−2.61 (m, 2H, CH$_2$), 2.39−2.24 (m, 1H, CH), 2.11 (d, J = 7.0 Hz, 2H, CH$_2$), 1.90−1.82 (m, 2H, CH$_2$), 1.80−1.59 (m, 3H, CH$_2$ + CH), 1.37 (s, 9H, C(CH$_3$)$_3$), 1.18 (t, J = 7.0 Hz, 3H, -OCH$_2$CH$_3$), 1.11−1.03 (m, 2H, CH$_2$), 0.99−0.92 (m, 2H, CH$_2$); ^{13}C NMR (151 MHz, CDCl$_3$) δ 173.1 (-NH-C=O), 156.3 (C=O), 79.3 (C(CH$_3$)$_3$), 60.3 (-CO$_2$CH$_2$CH$_3$), 56.6 (CH), 46.4 (CH$_2$), 41.8 (CH$_2$), 34.7 (CH), 33.3 (CH$_2$), 31.7 (CH$_2$), 28.6 (C(CH$_3$)$_3$), 14.4 (-CO$_2$CH$_2$CH$_3$); ν_{max}/cm (neat): 3348, 2953, 2851, 1731, 1711, 1520, 1450, 1391, 1282, 1249, 1172, 1032; HRMS (ESI-TOF) calcd for C$_{17}$H$_{33}$O$_4$N$_2$ [M + H]$^+$: 329.24348, found: 329.24289.

Ethyl 2-(trans-4-((tert-butoxycarbonyl)(2-((tert-butoxycarbonyl)-amino)ethyl)amino)cyclohexyl)acetate (10). Ethyl 2-(*trans*-4-((2-((*tert*-butoxycarbonyl)amino)ethyl)amino)cyclohexyl)acetate **9** (1.4 g, 4.26 mmol, 1 equiv) was dissolved in anhydrous CH$_2$Cl$_2$ (37 mL) before di-*tert*-butyl dicarbonate (2326 mg, 10.7 mmol, 2.5 equiv) and *N,N*-diisopropylethylamine (1.11 mL, 6.39 mmol, 1.5 equiv) were added. The reaction mixture was refluxed for 16 h, before the volatiles were removed in vacuo. The residue thus obtained was resuspended in CH$_2$Cl$_2$ (30 mL), and sat. aq NH$_4$Cl (50 mL) was added. The layers were separated, and the aqueous layer was extracted with CH$_2$Cl$_2$ (3 × 70 mL). The combined organic layers were dried (MgSO$_4$), then concentrated in vacuo. The crude material was purified by flash

chromatography (0−20% MeOH in CH$_2$Cl$_2$) to afford the desired product **10** as a yellow oil (1.50 g, 82%). R_f 0.90 (1:1 EtOAc−pentane); ^{1}H NMR (400 MHz, CDCl$_3$) δ 4.11 (q, J = 7.0 Hz, 2H, -OCH$_2$CH$_3$), 3.31−3.10 (m, 4H, CH$_2$), 2.17 (d, J = 7.0 Hz, 2H, CH$_2$), 1.86−1.58 (m, 5H, CH$_2$ + CH), 1.65−1.32 (m, 19H, C(CH$_3$)$_3$) + CH), 1.25 (t, J = 7.0, 3.0 Hz, 3H, -OCH$_2$CH$_3$), 1.17−0.99 (m, 2H, CH$_2$); ^{13}C NMR (101 MHz, CDCl$_3$) δ 172.8 (-NH-C=O), 156.4 (C=O), 156.1 (C=O), 79.9 (C(CH$_3$)$_3$), 60.2 (-CO$_2$CH$_2$CH$_3$), 42.5 (CH$_2$), 41.6 (CH), 41.0 (CH$_2$), 34.0 (CH), 32.2 (CH$_2$), 30.3 (CH$_2$), 28.5 (C(CH$_3$)$_3$), 28.4 (C(CH$_3$)$_3$), 14.3 (-CO$_2$CH$_2$CH$_3$); ν_{max}/cm (neat): 3367, 2978, 2931, 1715, 1689, 1516, 1453, 1408, 1391, 1248, 1170; HRMS (ESI-TOF) calcd for C$_{22}$H$_{41}$O$_6$N$_2$ [M + H]$^+$: 429.29591, found: 429.29582.

2-(trans-4-((tert-Butoxycarbonyl)(2-((tert-butoxycarbonyl)-amino)ethyl)amino)cyclohexyl)acetic Acid (11). Ethyl ester **10** (1604 mg, 3.74 mmol, 1 equiv) was dissolved in 1:2:1 mixture of THF/EtOH/H$_2$O (10 mL), and LiOH·H$_2$O (224 mg, 9.36 mmol, 2.5 equiv) was added. The resultant cloudy solution was stirred at rt for 5 h before the volatiles were removed in vacuo. The residue thus obtained was dissolved in minimum amount of water and filtered through a short column of *Amberlite* IR-120 (H$^+$ form). To the obtained aqueous filtrate was added EtOAc (50 mL), and the layers were separated. The aqueous layer was extracted with EtOAc (3 × 50 mL), washed with brine (20 mL), dried (Na$_2$SO$_4$), and then concentrated in vacuo to afford the desired product **11** as a shiny white solid (1 g, 67%). R_f 0.45 (1:1 EtOAc−pentane); mp 97−98 °C; ^{1}H NMR (500 MHz, CDCl$_3$) δ 3.36−3.12 (m, 4H, CH$_2$), 2.25 (d, J = 7.0 Hz, 2H, CH$_2$), 1.93−1.86 (m, 2H, CH$_2$), 1.80−1.70 (m, 3H, CH$_2$ + CH), 1.68−1.33 (m, 21H, C(CH$_3$)$_3$ + CH$_2$ + CH), 1.20−1.06 (m, 2H, CH$_2$); ^{13}C NMR (126 MHz, CDCl$_3$) δ 178.5 (C=O), 177.0 (C=O), 80.1 (C(CH$_3$)$_3$), 80.0 (C(CH$_3$)$_3$), 41.1 (CH$_2$), 33.7 (CH), 32.1 (CH$_2$), 30.3 (CH$_2$), 28.5 (C(CH$_3$)$_3$), 28.4 (C(CH$_3$)$_3$), 20.7; ν_{max}/cm (neat): 3055, 3009, 2974, 2930, 1706, 1686, 1672, 1518, 1477, 1409, 1365, 1247, 1023; HRMS (ESI-TOF) calcd for C$_{20}$H$_{37}$O$_6$N$_2$ [M + H]$^+$: 401.26461, found: 401.26401.

tert-Butyl 3-((R)-2-(2-(trans-4-((tert-butoxycarbonyl)(2-((tert-butoxycarbonyl)amino)ethyl)amino)cyclohexyl)acetamido)-2-((3aR,4R,6R,7aS)-3a,5,5-trimethylhexahydro-4,6-methanobenzo-[d][1,3,2]dioxaborol-2-yl)ethyl)-2-methoxybenzoate (12). To a solution of carboxylic acid **11** (416 mg, 1.04 mmol, 1.2 equiv) in anhydrous CH$_2$Cl$_2$ (2.60 mL) were added triethylamine (0.36 mL, 2.61 mmol, 3 equiv), benzotriazol-1-yl-oxytripyrrolidinophosphonium hexafluorophosphate (PyBOP; 541 mg, 1.04 mmol, 1.2 equiv), and crude amine **7** (325 mg, 0.87 mmol, 1 equiv). The resultant solution was stirred at rt for 75 min before water (10 mL) was added, and the layers were separated. The aqueous layer was extracted with CH$_2$Cl$_2$ (3 × 10 mL). The combined organic layers were washed with brine (10 mL), dried (MgSO$_4$), then concentrated in vacuo. The crude material was purified by flash chromatography (0−20% MeOH in CH$_2$Cl$_2$). Although several impurities were still present after this step (as judged by ^{1}H NMR and LC−MS), the amide **12** thus obtained as a yellow foam (224 mg, 34%) was used in the next step without further purification. R_f 0.55 (1:2 EtOAc−pentane); ^{1}H NMR (500 MHz, MeOD) δ 7.61−7.49 (m, 1H, Ar), 7.46−7.35 (m, 1H, Ar), 7.13−7.09 (m, 1H, Ar), 4.22−4.14 (m, 1H, CHOB), 3.80 (s, 3H, −OCH$_3$), 3.21−3.10 (m, 4H, −NCH$_2$CH$_2$NHBoc), 2.94−2.85 (m, 2H, CHB + Ar-CH$_2$), 2.75−2.67 (m, 1H, Ar-CH$_2$), 2.38−2.30 (m, 1H, pinanediol-CH$_2$), 2.26 (d, J = 7.0 Hz, 2H, -CHCH$_2$CO), 2.12−2.06 (m, 1H, pinanediol-CH$_2$), 2.01 (s, 1H, cyclohexyl-CH), 1.94 (app t, J = 5.5 Hz, 1H, pinanediol-CH), 1.90−1.79 (m, 5H, cyclohexyl-CH$_2$ + pinanediol-CH), 1.76−1.66 (m, 3H, cyclohexyl-CH$_2$ + cyclohexyl-CH), 1.64−1.58 (m, 11H, -CO$_2$C-(CH$_3$)$_3$ + cyclohexyl-CH$_2$), 1.40−1.36 (s, 10H, C(CH$_3$)$_3$ + pinanediol-CH$_2$), 1.43 (s, 9H, C(CH$_3$)$_3$), 1.37 (s, 3H, CH$_3$), 1.28 (s, 3H, CH$_3$), 1.18−1.08 (m, 2H, cyclohexyl-CH$_2$), 0.89 (s, 3H, CH$_3$); ^{13}C NMR (126 MHz, MeOD) δ 174.9, 173.0, 170.3, 158.4, 157.3, 144.1, 141.5, 133.2, 131.1, 130.3, 126.5, 125.6, 124.7, 81.2, 80.0, 78.4, 69.9, 61.5, 59.8, 55.3, 52.9, 51.9, 42.0, 41.8, 40.8, 38.7, 36.8, 35.2, 33.2, 30.1, 29.1, 29.0, 28.8, 28.7, 28.4, 28.4, 27.5, 27.2, 24.6, 24.3, 20.9, 14.5; ν_{max}/cm (neat): 3627, 3599, 2987, 2864, 2360, 1701, 1692, 1592, 1466, 1454, 1305, 1277, 1136; HRMS (ESI-TOF) calcd for C$_{44}$H$_{71}$O$_{10}$N$_3$^{10}B [M + H]$^+$: 811.52633, found: 811.52667.

(R)-3-(2-(trans-4-((2-Aminoethyl)amino)cyclohexyl)acetamido)-2-hydroxy-3,4-dihydro-2H-benzo[e][1,2]oxaborinine-8-carboxylic Acid (13). To a precooled (−78 °C) solution of boronate **12** (50 mg, 0.06 mmol, 1 equiv) in anhydrous CH_2Cl_2 (1 mL) was added BCl_3 (1 M in CH_2Cl_2, 0.31 mL, 5 equiv) dropwise over 20 min. The reaction mixture was stirred for 60 min, then water (5 mL) was added, and the layers were separated. The organic layer was extracted with water (3 × 5 mL). The combined aqueous layers were lyophilized to afford the crude product as a brown solid. Following challenging purification via HPLC preparatory method A, the desired product **13** was obtained as a white solid (10 mg, 42%). The relatively low yield may reflect deborylation during purification as suggested by LC−MS analyses of the collected fractions. Purity: ≥96% by qHNMR; R_f baseline (1:1 CH_2Cl_2−MeOH); ^{1}H NMR (600 MHz, D_2O) δ 7.84−7.75 (m, 1H, H-4), 7.47−7.37 (m, 1H, H-6), 7.06 (app t, J = 8.0 Hz, 1H, H-5), 3.34−3.29 (m, 4H, H-33, H-34), 3.28−3.22 (m, 1H, H-9), 3.00−2.88 (m, 2H, H-8), 2.82−2.71 (m, 1H, H-23), 2.34−2.27 (m, 1H, H-19′), 2.14−2.04 (m, 1H, H-19″), 1.88−1.73 (m, 2H, C$\underline{H}_2$-27/C$\underline{H}_2$-29), 1.43−1.37 (m, 1H, C$\underline{H}_2$-26/C$\underline{H}_2$-30), 1.35−1.26 (m, 1H, H-25), 1.20−0.90 (m, 2H, C$\underline{H}_2$-27/C$\underline{H}_2$-29), 0.86−0.75 (m, 1H, C$\underline{H}_2$-26/C$\underline{H}_2$-30), 0.68−0.38 (m, 2H, C$\underline{H}_2$-26/C$\underline{H}_2$-30); ^{13}C NMR (151 MHz, D_2O) δ 179.3 (C-10), 169.93 (C-3), 156.4 (C-1), 136.6 (C-6), 129.7 (C-4), 128.7 (Ar-$\underline{C}$), 121.9 (C-5), 116.7 (Ar-$\underline{C}$), 56.9 (C-23), 41.1 (C-33/C-34), 35.6 (C-33/C-34), 35.5 (C-19), 33.6 (C-25), 30.5 (C-8), 28.9 (C-26/C-30), 28.4 (C-26/C-30), 28.1 (C-27/C-39), 28.0 (C-27/C-39), C-9 not observed due to peak broadening; HRMS (ESI-TOF) calcd for $C_{19}H_{29}O_5N_3{}^{10}B$ [M + H]$^+$: 389.22311, found: 389.22333.

Inhibition Assays. Inhibitory activity of VNRX-5133 against representative SBLs and MBLs was determined using a fluorogenic assay monitoring the enzymatic breakdown of the cephalosporin probe FC5,[38] with the exception of the subclass B2 MBL CphA, for which the hydrolysis of meropenem substrate was used.[27] The FC5/meropenem assays were conducted at room temperature in clear-bottomed Greiner 384 black well microplates (FC5) or Greiner 96 well UV star microplates (meropenem), using a ClarioStar or PHERAstar FS microplate reader (BMG LabTech). Representative β-lactamases were tested at the following concentrations: AmpC, 500 pM; OXA-10, 250 pM; OXA-48, 12.5 nM; TEM, 1 nM; VIM-1, 100 pM; NDM-1, 20 pM; IMP-1, 20 pM; VIM-2, 500 pM; and L1, 50 pM. The concentration of FC5 employed was 10 μM for TEM-1 and 5 μM for all other enzymes. The concentration of meropenem used was 12.5 μM for CphA. TEM-116, AmpC, OXA-10, and OXA-48 inhibition assays were run in "SBL buffer" (phosphate buffer, pH 7.4, 0.01% (v/v) Triton X-100), while IMP-1, VIM-1, VIM-2, NDM-1, NDM-2, L1, and CphA were screened in "MBL buffer" (50 mM HEPES, pH 7.2, 1 μM $ZnSO_4$, 1 μg mL^{-1} BSA, 0.01% v/v Triton X-100). OXA-10 and OXA-48 assays were also run in "SBL buffer" supplemented with 100 mM $NaHCO_3$. The initial rates of reaction (measured after 10 min pre-incubation of VNRX-5133 with the enzyme) were assessed by monitoring the fluorescence intensity at λ_{ex} = 380 nm and λ_{em} = 460 nm, except for B2 MBL CphA, where UV absorbance was monitored at λ = 300 nm. Following the determination of initial rates of reaction, the data were fitted using a four-parameter function: log (inhibitor) vs. response, variable slope in GraphPad Prism 6 (Supporting Information Table S1) to obtain IC$_{50}$ values.

Antimicrobial Susceptibility Testing. Meropenem (MEM) and cefepime (Cef) were tested alone (0.06−64 μg mL^{-1}) and in combination with bicyclic boronate VNRX-5133 (10 μg mL^{-1}) against a small set of NDM-1-producing *Enterobacteriaceae* (Table 2), in triplicate. Minimal inhibitory concentration (MIC) values were determined by the agar dilution method and interpreted using published guidelines described by EUCAST/CLSI.[57] All reported MIC values are within ±1 log$_2$ dilution of the reference MIC values.

Crystallization Experiments, X-ray Data Collection, and Processing. NDM-1 was cloned and purified as previously described.[28] Crystallization experiments were set up using a solution of OXA-10 (8.5 mg mL^{-1}) in 50 mM MES, pH 6.0; 100 mM NaCl; and NDM-1 (30 mg mL^{-1}) in 20 mM Tris, pH 8.0; 150 mM NaCl; and 2 mM DTT. OXA-10 crystals were supplemented with 10 mM VNRX-5133. OXA-10 crystallization was performed at room temperature using

the sitting drop vapor diffusion method. Crystals were obtained using 100 μL of reservoir solution, i.e. 200 mM $Zn(OAc)_2\cdot2H_2O$, 100 mM imidazole, 20% PEG 3000, pH 8.0, and a 1:1 mixture (0.2 μL:0.2 μL) of protein/reservoir solution in the crystallization drop. Crystals were cryoprotected using well solution diluted to 25% (v/v) aqueous glycerol and harvested with nylon loops and subsequent flash-cooling in liquid nitrogen.

NDM-1 was crystallized by sitting drop vapor diffusion in CrysChem 24-well plates (Hampton Research) at 19 °C, with micro seeding. Protein (2 μL) was mixed with 1.5 μL of the reservoir solution (32% PEG3350, 0.1 M Bis-Tris, pH 5.8, 0.15 M NH_4SO_4) and 0.5 μL of crystal seed. Crystals were then soaked by addition of 2 mM VNRX-5133 directly to the drop for 4 h. Crystals were then cryoprotected by brief exposure to 20% (v/v) aqueous glycerol (in well solution) and subsequently flash-cooled in liquid nitrogen.

Diffraction data for OXA-10 and NDM-1 were collected at 100 K at beamlines I04 and I24, respectively, of the Diamond Light Source, Didcot. OXA-10 diffraction data were integrated and scaled using autoPROC. NDM-1 data were integrated in DIALS and scaled in Aimless. The structures were solved by isomorphous molecular replacement using reported NDM-1 (PDB accession code: 3SPU[58]) and OXA-10 (PDB accession code: 5FQ9[27]) as search models. Both structures were then iteratively fitted and refined using PHENIX[59] and Coot.[60] Processing and refinement statistics for NDM-1 and OXA-10 with VNRX-5133 can be found in Supporting Information Table S3. Molprobity validation reports for OXA-10 and NDM-1 structures are available in Supporting Information Tables S4 and S5, respectively.

■ ASSOCIATED CONTENT

Ⓢ Supporting Information
The Supporting Information is available free of charge on the ACS Publications website at DOI: 10.1021/acs.jmedchem.9b00911.

> Molecular formula strings for VNRX-5133 (CSV)
> ^{1}H NMR, ^{13}C NMR, and HRMS spectra of all synthesized compounds; LC−MS spectrum of VNRX-5133; data from time dependence experiments; error analysis for reported inhibition values and processing and refinement statistics (including Molprobity validation reports) (PDF)

Accession Codes
Coordinates and structure factors have been deposited in the Protein Data Bank under accession codes 6RMF (NDM-1:**VNRX-5133**) and 6RTN (OXA-10:**VNRX-5133**). Authors will release the atomic coordinates and experimental data upon article publication.

■ AUTHOR INFORMATION

Corresponding Author
*E-mail: christopher.schofield@chem.ox.ac.uk. Tel: +44 (0) 1865 275625. Fax: +44 (0)1865 285002.

ORCID Ⓞ
Alen Krajnc: 0000-0001-7822-1944
Jürgen Brem: 0000-0002-0137-3226
Philip Hinchliffe: 0000-0001-8611-4743
Pauline A. Lang: 0000-0003-3187-1469
James Spencer: 0000-0002-4602-0571
Christopher J. Schofield: 0000-0002-0290-6565

Author Contributions
C.J.S. and J.B. conceived the research. A.K. with the help of TDP synthesized and characterized compounds used for the study. J.B., K.C., P.A.L., and J.A.G.K. purified the enzymes used in biochemical studies (except NDM-1 used for crystallography), crystallized VNRX-5133 with OXA-10, collected X-ray data, and

solved the structure. P.H. and J.S. crystallized VNRX-5133 with NDM-1 and carried out the crystallographic analysis. J.M.T., E.W., and T.R.W. performed the MIC experiments. B.G.S. assisted A.K. with the HPLC purification. A.K. and C.J.S. wrote the initial drafts of the manuscript. A.K., J.B., P.H., and C.J.S. discussed the results and wrote the final manuscript. All authors provided feedback and helped shape the manuscript.

Notes

The authors declare no competing financial interest.

◾ ABBREVIATIONS

SBL, serine-β-lactamase; MBL, metallo-β-lactamase; ESBL, extended-spectrum β-lactamase; PBP, penicillin-binding protein; PDB, Protein Data Bank; DMF, dimethylformamide; HEPES, (4-(2-hydroxyethyl)-1-piperazineethanesulfonic acid; UV, ultraviolet; THF, tetrahydrofuran; rt, room temperature; PyBOP, benzotriazol-1-yl-oxytripyrrolidinophosphonium hexafluorophosphate; HPLC, high-performance liquid chromatography; NMR, nuclear magnetic resonance; Boc, *tert*-butoxycarbonyl; IC$_{50}$, half-maximal inhibitory concentration; Ec, Escherichia coli; Kp, Klebsiella pneumoniae; MIC, minimal inhibitory concentration; MEM, meropenem; Cef, cefepime; MES, 2-(N-morpholino)ethanesulfonic acid; Tris, tris-(hydroxymethyl)aminomethane; DTT, dithiothreitol; PEG, poly(ethylene glycol)

◾ REFERENCES

(1) Munita, J. M.; Arias, C. A. Mechanisms of Antibiotic Resistance. *Microbiol. Spectr.* **2016**, *4*, No. 42.

(2) Majiduddin, F. K.; Materon, I. C.; Palzkill, T. G. Molecular analysis of beta-lactamase structure and function. *Int. J. Med. Microbiol.* **2002**, *292*, 127−137.

(3) Leigh, D. A.; Bradnock, K.; Marriner, J. M. Augmentin (amoxycillin and clavulanic acid) therapy in complicated infections due to beta-lactamase producing bacteria. *J. Antimicrob. Chemother.* **1981**, *7*, 229−236.

(4) Reading, C.; Cole, M. Clavulanic acid: a beta-lactamase-inhiting beta-lactam from Streptomyces clavuligerus. *Antimicrob. Agents Chemother.* **1977**, *11*, 852−857.

(5) Benson, J. M.; Nahata, M. C. Sulbactam/ampicillin, a new beta-lactamase inhibitor/beta-lactam antibiotic combination. *Drug Intell. Clin. Pharm.* **1988**, *22*, 534−541.

(6) Gutmann, L.; Kitzis, M. D.; Yamabe, S.; Acar, J. F. Comparative evaluation of a new beta-lactamase inhibitor, YTR 830, combined with different beta-lactam antibiotics against bacteria harboring known beta-lactamases. *Antimicrob. Agents Chemother.* **1986**, *29*, 955−957.

(7) Papp-Wallace, K. M.; Endimiani, A.; Taracila, M. A.; Bonomo, R. A. Carbapenems: past, present, and future. *Antimicrob. Agents Chemother.* **2011**, *55*, 4943−4960.

(8) Bush, K.; Bradford, P. A. Interplay between beta-lactamases and new beta-lactamase inhibitors. *Nat. Rev. Microbiol.* **2019**, *17*, 295−306.

(9) Palzkill, T. Metallo-beta-lactamase structure and function. *Ann. N. Y. Acad. Sci.* **2013**, *1277*, 91−104.

(10) Walsh, T. R. Emerging carbapenemases: a global perspective. *Int. J. Antimicrob. Agents* **2010**, *36*, S8−S14.

(11) Zhanel, G. G.; Lawson, C. D.; Adam, H.; Schweizer, F.; Zelenitsky, S.; Lagace-Wiens, P. R.; Denisuik, A.; Rubinstein, E.; Gin, A. S.; Hoban, D. J.; Lynch, J. P., 3rd; Karlowsky, J. A. Ceftazidime-avibactam: a novel cephalosporin/beta-lactamase inhibitor combination. *Drugs* **2013**, *73*, 159−177.

(12) Ehmann, D. E.; Jahic, H.; Ross, P. L.; Gu, R. F.; Hu, J.; Kern, G.; Walkup, G. K.; Fisher, S. L. Avibactam is a covalent, reversible, non-beta-lactam beta-lactamase inhibitor. *Proc. Natl. Acad. Sci. U.S.A.* **2012**, *109*, 11663−11668.

(13) Abboud, M. I.; Damblon, C.; Brem, J.; Smargiasso, N.; Mercuri, P.; Gilbert, B.; Rydzik, A. M.; Claridge, T. D. W.; Schofield, C. J.; Frère, J.-M. Interaction of Avibactam with Class B Metallo-β-Lactamases. *Antimicrob. Agents Chemother.* **2016**, *60*, 5655−5662.

(14) Lohans, C. T.; Brem, J.; Schofield, C. J. New Delhi Metallo-β-Lactamase 1 Catalyzes Avibactam and Aztreonam Hydrolysis. *Antimicrob. Agents Chemother.* **2017**, *61*, e01224−e01217.

(15) Gareth, W.; Langley, R. C.; Tyrrell, J. M.; Hinchliffe, P.; Calvopiña, K.; Tooke, C.; Widlake, E.; Dowson, C. G.; Spencer, J.; Walsh, T. R.; Schofield, C. J.; Brem, J. Profiling Interactions of Vaborbactam with Metallo-β-Lactamases. *Bioorg. Med. Chem. Lett.* **2019**, *29*, 1981−1984.

(16) Field-Smith, A.; Morgan, G. J.; Davies, F. E. Bortezomib (Velcade trade mark) in the Treatment of Multiple Myeloma. *Ther. Clin. Risk Manage.* **2006**, *2*, 271−279.

(17) Morandi, F.; Caselli, E.; Morandi, S.; Focia, P. J.; Blazquez, J.; Shoichet, B. K.; Prati, F. Nanomolar inhibitors of AmpC beta-lactamase. *J. Am. Chem. Soc.* **2003**, *125*, 685−695.

(18) Werner, J. P.; Mitchell, J. M.; Taracila, M. A.; Bonomo, R. A.; Powers, R. A. Exploring the potential of boronic acids as inhibitors of OXA-24/40 beta-lactamase. *Protein Sci.* **2017**, *26*, 515−526.

(19) Rojas, L. J.; Taracila, M. A.; Papp-Wallace, K. M.; Bethel, C. R.; Caselli, E.; Romagnoli, C.; Winkler, M. L.; Spellberg, B.; Prati, F.; Bonomo, R. A. Boronic Acid Transition State Inhibitors Active against KPC and Other Class A beta-Lactamases: Structure-Activity Relationships as a Guide to Inhibitor Design. *Antimicrob. Agents Chemother.* **2016**, *60*, 1751−1759.

(20) Strynadka, N. C.; Martin, R.; Jensen, S. E.; Gold, M.; Jones, J. B. Structure-based design of a potent transition state analogue for TEM-1 beta-lactamase. *Nat. Struct. Mol. Biol.* **1996**, *3*, 688−695.

(21) Ness, S.; Martin, R.; Kindler, A. M.; Paetzel, M.; Gold, M.; Jensen, S. E.; Jones, J. B.; Strynadka, N. C. Structure-based design guides the improved efficacy of deacylation transition state analogue inhibitors of TEM-1 beta-Lactamase. *Biochemistry* **2000**, *39*, 5312−5321.

(22) Diaz, D. B.; Yudin, A. K. The versatility of boron in biological target engagement. *Nat. Chem.* **2017**, *9*, 731−742.

(23) Krajnc, A.; Lang, P. A.; Panduwawala, T. D.; Brem, J.; Schofield, C. J. Will morphing boron-based inhibitors beat the beta-lactamases? *Curr. Opin. Chem. Biol.* **2019**, *50*, 101−110.

(24) Hecker, S. J.; Reddy, K. R.; Totrov, M.; Hirst, G. C.; Lomovskaya, O.; Griffith, D. C.; King, P.; Tsivkovski, R.; Sun, D.; Sabet, M.; Tarazi, Z.; Clifton, M. C.; Atkins, K.; Raymond, A.; Potts, K. T.; Abendroth, J.; Boyer, S. H.; Loutit, J. S.; Morgan, E. E.; Durso, S.; Dudley, M. N. Discovery of a Cyclic Boronic Acid beta-Lactamase Inhibitor (RPX7009) with Utility vs Class A Serine Carbapenemases. *J. Med. Chem.* **2015**, *58*, 3682−3692.

(25) Dhillon, S. Meropenem/Vaborbactam: A Review in Complicated Urinary Tract Infections. *Drugs* **2018**, *78*, 1259−1270.

(26) Lomovskaya, O.; Sun, D.; Rubio-Aparicio, D.; Nelson, K.; Tsivkovski, R.; Griffith, D. C.; Dudley, M. N. Vaborbactam: Spectrum

of Beta-Lactamase Inhibition and Impact of Resistance Mechanisms on Activity in Enterobacteriaceae. *Antimicrob. Agents Chemother.* **2017**, *61*, e01443−e01417.

(27) Brem, J.; Cain, R.; Cahill, S.; McDonough, M. A.; Clifton, I. J.; Jiménez-Castellanos, J.-C.; Avison, M. B.; Spencer, J.; Fishwick, C. W. G.; Schofield, C. J. Structural basis of metallo-*β*-lactamase, serine-*β*-lactamase and penicillin-binding protein inhibition by cyclic boronates. *Nat. Commun.* **2016**, *7*, No. 12406.

(28) Cahill, S. T.; Cain, R.; Wang, D. Y.; Lohans, C. T.; Wareham, D. W.; Oswin, H. P.; Mohammed, J.; Spencer, J.; Fishwick, C. W. G.; McDonough, M. A.; Schofield, C. J.; Brem, J. Cyclic Boronates Inhibit All Classes of *β*-Lactamases. *Antimicrob. Agents Chemother.* **2017**, *61*, e02260−e02216.

(29) Cahill, S. T.; Tyrrell, J. M.; Navratilova, I. H.; Calvopina, K.; Robinson, S. W.; Lohans, C. T.; McDonough, M. A.; Cain, R.; Fishwick, C. W. G.; Avison, M. B.; Walsh, T. R.; Schofield, C. J.; Brem, J. Studies on the inhibition of AmpC and other beta-lactamases by cyclic boronates. *Biochim. Biophys. Acta, Gen. Subj.* **2019**, *1863*, 742−748.

(30) Burns, C. J.; Daigle, D.; Liu, B.; McGarry, D.; Pevear, D. C.; Trout, R. E. L. Beta-Lactamase Inhibitors. WO Patent WO 2014/089365 A1.

(31) Mushtaq, S.; Vickers, A.; Woodford, N.; Livermore, D. M. *Potentiation of cefepime by the boronate VNRX-5133 versus gram-negative bacteria with known β-lactamases*; European Congress of Clinical Microbiology and Infectious Diseases (ECCMID) in Madrid: Spain, 2018.

(32) Hackel Meredith, D. S. *Antimicrobial Activity of Cefepime in Combination with VNRX-5133 Against a Global 2018 Surveillance Collection of Clinical Isolates*; European Congress of Clinical Microbiology and Infectious Diseases (ECCMID) in Amsterdam: The Netherlands, 2019.

(33) Hamrick, J. C.; Chatwin, C. L.; John, K. J.; Pevear, D. C.; Burns, C. J.; Xerri, L. *The Ability of Broad-spectrum β-Lactamase Inhibitor Vnrx-5133 to Restore Bactericidal Activity of Cefepime in Enterobacteriaceae and P. aeruginosa-Expressing Ambler Class A, B, C and D Enzymes is Demonstrated Using Time-Kill Kinetics*; European Congress of Clinical Microbiology and Infectious Diseases (ECCMID) in Madrid: Spain, 2018.

(34) Matteson, D. S. Boronic esters in asymmetric synthesis. *J. Org. Chem.* **2013**, *78*, 10009−10023.

(35) Matteson, D. S.; Majumdar, D. Homologation of Boronic Esters to Alpha-Chloro Boronic Esters. *Organometallics* **1983**, *2*, 1529−1535.

(36) Matteson, D. S.; Ray, R. Directed Chiral Synthesis with Pinanediol Boronic Esters. *J. Am. Chem. Soc.* **1980**, *102*, 7590−7591.

(37) Coste, J.; Le-Nguyen, D.; Castro, B. PyBOP: A new peptide coupling reagent devoid of toxic by-product. *Tetrahedron Lett.* **1990**, *31*, 205−208.

(38) van Berkel, S. S.; Brem, J.; Rydzik, A. M.; Salimraj, R.; Cain, R.; Verma, A.; Owens, R. J.; Fishwick, C. W.; Spencer, J.; Schofield, C. J. Assay platform for clinically relevant metallo-beta-lactamases. *J. Med. Chem.* **2013**, *56*, 6945−6953.

(39) Daigle, D.; Hamrick, J.; Chatwin, C.; Kurepina, N.; Kreiswirth, B. N.; Shields, R. K.; Oliver, A.; Clancy, C. J.; Nguyen, M.-H.; Pevear, D.; Xerri, L. 1370. Cefepime/VNRX-5133 Broad-Spectrum Activity Is Maintained Against Emerging KPC- and PDC-Variants in Multidrug-Resistant *K. pneumoniae* and *P. aeruginosa*. *Open Forum Infect. Dis.* **2018**, *5*, S419−S420.

(40) van den Akker, F.; Bonomo, R. A. Exploring Additional Dimensions of Complexity in Inhibitor Design for Serine *β*-Lactamases: Mechanistic and Intra- and Inter-molecular Chemistry Approaches. *Front. Microbiol.* **2018**, *9*, 1−622.

(41) Calvopiña, K.; Hinchliffe, P.; Brem, J.; Heesom, K. J.; Johnson, S.; Cain, R.; Lohans, C. T.; Fishwick, C. W. G.; Schofield, C. J.; Spencer, J.; Avison, M. B. Structural/mechanistic insights into the efficacy of nonclassical beta-lactamase inhibitors against extensively drug resistant *Stenotrophomonas maltophilia* clinical isolates. *Mol. Microbiol.* **2017**, *106*, 492−504.

(42) Inglis, S. R.; Woon, E. C. Y.; Thompson, A. L.; Schofield, C. J. Observations on the Deprotection of Pinanediol and Pinacol Boronate Esters via Fluorinated Intermediates. *J. Org. Chem.* **2010**, *75*, 468−471.

(43) Zhang, H.; Ma, G.; Zhu, Y.; Zeng, L.; Ahmad, A.; Wang, C.; Pang, B.; Fang, H.; Zhao, L.; Hao, Q. Active-Site Conformational Fluctuations Promote the Enzymatic Activity of NDM-1. *Antimicrob. Agents Chemother.* **2018**, *62*, e01579−e01518.

(44) Ullah, J. H.; Walsh, T. R.; Taylor, I. A.; Emery, D. C.; Verma, C. S.; Gamblin, S. J.; Spencer, J. The crystal structure of the L1 metallo-*β*-lactamase from *Stenotrophomonas maltophilia* at 1.7 å resolution11 Edited by K. Nagai. *J. Mol. Biol.* **1998**, *284*, 125−136.

(45) Hopkinson, R. J.; Tumber, A.; Yapp, C.; Chowdhury, R.; Aik, W.; Che, K. H.; Li, X. S.; Kristensen, J. B. L.; King, O. N. F.; Chan, M. C.; Yeoh, K. K.; Choi, H.; Walport, L. J.; Thinnes, C. C.; Bush, J. T.; Lejeune, C.; Rydzik, A. M.; Rose, N. R.; Bagg, E. A.; McDonough, M. A.; Krojer, T.; Yue, W. W.; Ng, S. S.; Olsen, L.; Brennan, P. E.; Oppermann, U.; Muller-Knapp, S.; Klose, R. J.; Ratcliffe, P. J.; Schofield, C. J.; Kawamura, A. 5-Carboxy-8-hydroxyquinoline is a Broad Spectrum 2-Oxoglutarate Oxygenase Inhibitor which Causes Iron Translocation. *Chem. Sci.* **2013**, *4*, 3110−3117.

(46) Tierney, D. L.; Schenk, G. X-ray absorption spectroscopy of dinuclear metallohydrolases. *Biophys. J.* **2014**, *107*, 1263−1272.

(47) Aitha, M.; Al-Adbul-Wahid, S.; Tierney, D. L.; Crowder, M. W. Probing substrate binding to the metal binding sites in metallo-*β*-lactamase L1 during catalysis. *MedChemComm* **2016**, *7*, 194−201.

(48) Gonzalez, M. M.; Kosmopoulou, M.; Mojica, M. F.; Castillo, V.; Hinchliffe, P.; Pettinati, I.; Brem, J.; Schofield, C. J.; Mahler, G.; Bonomo, R. A.; Llarrull, L. I.; Spencer, J.; Vila, A. J. Bisthiazolidines: A Substrate-Mimicking Scaffold as an Inhibitor of the NDM-1 Carbapenemase. *ACS Infect. Dis.* **2015**, *1*, 544−554.

(49) Garau, G.; Bebrone, C.; Anne, C.; Galleni, M.; Frère, J.-M.; Dideberg, O. A Metallo-*β*-lactamase Enzyme in Action: Crystal Structures of the Monozinc Carbapenemase CphA and its Complex with Biapenem. *J. Mol. Biol.* **2005**, *345*, 785−795.

(50) Wu, S.; Xu, D.; Guo, H. QM/MM Studies of Monozinc *β*-Lactamase CphA Suggest That the Crystal Structure of an Enzyme−Intermediate Complex Represents a Minor Pathway. *J. Am. Chem. Soc.* **2010**, *132*, 17986−17988.

(51) Vercheval, L.; Bauvois, C.; di Paolo, A.; Borel, F.; Ferrer, J.-L.; Sauvage, E.; Matagne, A.; Frère, J.-M.; Charlier, P.; Galleni, M.; Kerff, F. Three factors that modulate the activity of class D *β*-lactamases and interfere with the post-translational carboxylation of Lys70. *Biochem. J.* **2010**, *432*, 495−506.

(52) Abdelraouf, K.; Abuhussain, S. A.; Nicolau, D. P. 1405. Efficacy of the Human-Simulated Regimen (HSR) of Cefepime (FEP)/VNRX-5133 Combination Against Serine *β*-Lactamase-Producing Gram-negative Bacteria in the Neutropenic Murine Thigh Infection Model. *Open Forum Infect. Dis.* **2018**, *5*, S432−S433.

(53) Geibel, B.; Dowell, J.; Dickerson, D.; Henkel, T. 1401. A Randomized, Double-Blind, Placebo-Controlled Study of the Safety and Pharmacokinetics of Single and Repeat Doses of VNRX-5133 in Healthy Subjects. *Open Forum Infect. Dis.* **2018**, *5*, S431.

(54) Hackel, M.; Sahm, D. 1360. Antimicrobial Activity of Cefepime in Combination with VNRX-5133 Against a Global Collection of Enterobacteriaceae Including Resistant Phenotypes. *Open Forum Infect. Dis.* **2018**, *5*, S416−S417.

(55) Demetriades, M.; Leung, I. K.; Chowdhury, R.; Chan, M. C.; McDonough, M. A.; Yeoh, K. K.; Tian, Y. M.; Claridge, T. D.; Ratcliffe, P. J.; Woon, E. C.; Schofield, C. J. Dynamic combinatorial chemistry employing boronic acids/boronate esters leads to potent oxygenase inhibitors. *Angew. Chem., Int. Ed.* **2012**, *51*, 6672−6675.

(56) Zervosen, A.; Herman, R.; Kerff, F.; Herman, A.; Bouillez, A.; Prati, F.; Pratt, R. F.; Frere, J. M.; Joris, B.; Luxen, A.; Charlier, P.; Sauvage, E. Unexpected tricovalent binding mode of boronic acids within the active site of a penicillin-binding protein. *J. Am. Chem. Soc.* **2011**, *133*, 10839−10848.

(57) Wayne, P. A. *Performance Standards for Antimicrobial Susceptibility Testing*, 27th ed.; Clinical and Laboratory Standards Institute, 2017.

(58) King, D.; Strynadka, N. Crystal structure of New Delhi metallo-beta-lactamase reveals molecular basis for antibiotic resistance. *Protein Sci.* **2011**, *20*, 1484−1491.

(59) Adams, P. D.; Grosse-Kunstleve, R. W.; Hung, L.-W.; Ioerger, T. R.; McCoy, A. J.; Moriarty, N. W.; Read, R. J.; Sacchettini, J. C.; Sauter, N. K.; Terwilliger, T. C. PHENIX: building new software for automated crystallographic structure determination. *Acta Crystallogr., Sect. D: Biol. Crystallogr.* **2002**, *58*, 1948−1954.

(60) Emsley, P.; Lohkamp, B.; Scott, W. G.; Cowtan, K. Features and development of Coot. *Acta Crystallogr., Sect. D: Biol. Crystallogr.* **2010**, *66*, 486−501.